

pubs.acs.org/NanoLett Letter

# Dipolar Ligands Tune Plasmonic Properties of Tin-Doped Indium Oxide Nanocrystals

Victor Segui Barragan, Benjamin J. Roman, Sofia A. Shubert-Zuleta, Marina W. Berry, Hugo Celio, and Delia J. Milliron\*



Cite This: Nano Lett. 2023, 23, 7983-7989



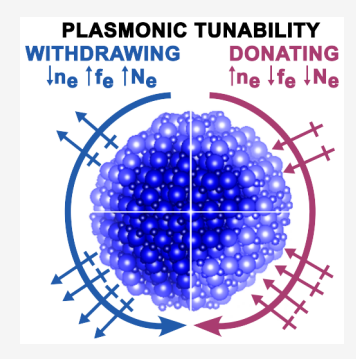
**ACCESS** 

III Metrics & More

Article Recommendations

s Supporting Information

ABSTRACT: Surface functionalization with dipolar molecules is known to tune the electronic band alignment in semiconductor films and colloidal quantum dots. Yet, the influence of surface modification on plasmonic nanocrystals and their properties remains little explored. Here, we functionalize tin-doped indium oxide nanocrystals (ITO NCs) via ligand exchange with a series of cinnamic acids with different electron-withdrawing and -donating dipolar characters. Consistent with previous reports on semiconductors, we find that withdrawing (donating) ligands increase (decrease) the work function caused by an electrostatic potential shift across the molecular layer. Quantitative analyses of the plasmonic extinction spectra reveal that varying the ligand molecular dipole affects the near-surface depletion layer, with an anticorrelated trend between the electron concentration and electronic volume fraction, factors that are positively correlated in assynthesized NCs. Electronic structure engineering through surface modification provides access to distinctive combinations of plasmonic properties that could enable optoelectronic applications, sensing, and hot electron-driven processes.



**KEYWORDS:** localized surface plasmon resonance, ligand exchange, band bending, electrostatics, infrared, ultraviolet photoemission spectroscopy

he influence of surfaces on all material properties is amplified for nanomaterials owing to their large specific surface areas. A powerful strategy for tuning the electronic properties of surfaces and interfaces is to introduce dipolar molecules that bind in an oriented manner to the surface of metals<sup>1</sup> and semiconductors,<sup>2</sup> modifying electronic properties such as the work function that is the energetic barrier to removing electrons from the material. Work function changes across a wide range of material compositions have been rationalized as due to the dipole of the molecules establishing a step in the potential energy of electrons as they cross the layer.<sup>3,4</sup> Withdrawing (donating) molecules consistently result in an increase (decrease) of the work function. 1,2,4-13 This approach has been used to engineer the band alignment at interfaces, raising or lowering the barriers to move electrons and holes between materials and strongly impacting optoelectronic properties in heterostructures ranging from metal/ semiconductor contacts to films of colloidal quantum dots, leading to more efficient light-emitting devices and solar cells.<sup>7,8,10,14,15</sup> Varying the dipole in a surface molecular layer can modify the built-in potential, or the extent of band bending in the near-surface region, 9,12 which controls the availability of photogenerated charge carriers for energy conversion or photocatalytic reactions. 16-18

Even though there has been considerable success in tuning the electronic properties of metal and semiconductor films, as well as colloidal nanomaterials, the influence of dipolar surface layers on plasmonic nanoparticles remains largely unexplored. In plasmonic nanoparticles, free charge carriers oscillate in response to light but are confined to the nanoparticles, resulting in strong absorption or scattering at a specific frequency known as the localized surface plasmon resonance (LSPR). The LSPR frequency is sensitive to the nanoparticle environment, so changes in surface chemistry are expected to influence plasmonic properties.<sup>19</sup> In a previous study, electrondonating and -withdrawing ligands were bound post-synthetically to gold nanoparticles, impacting their optical and electronic properties, yet the electrostatic effects of the molecular dipoles were not considered in the analysis, leaving open the question of how surface dipolar ligands influence plasmonic nanomaterials.<sup>20</sup> Furthermore, unlike conventional metals, plasmonic semiconductor nanocrystals (NCs) can be strongly influenced by a surface space charge layer, <sup>19,21–23</sup> and the interplay between surface dipole effects and band bending in governing their plasmonic properties is unknown. Therefore, we hypothesize that because molecular layers can modify the electronic properties at the surface of materials, using surface

Received: May 24, 2023 Revised: July 31, 2023 Published: August 25, 2023





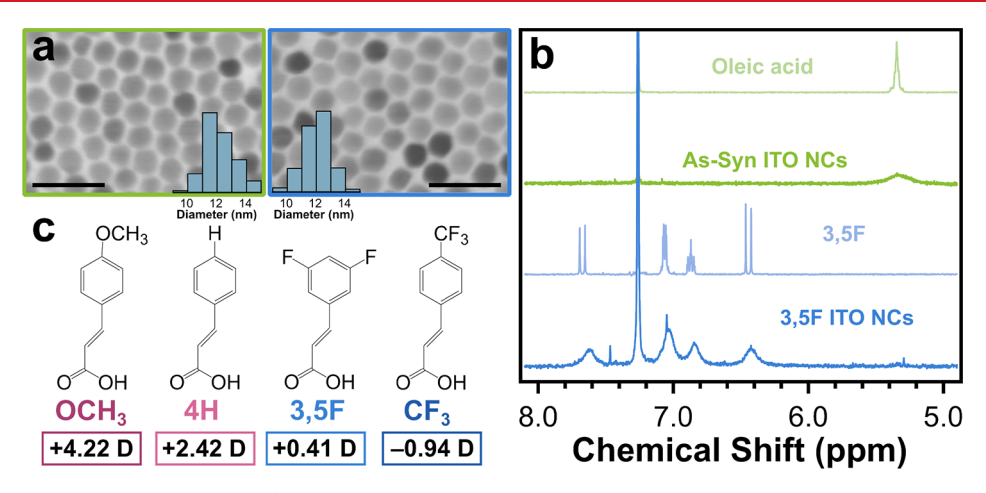


Figure 1. ITO NCs surface functionalization. (a) STEM images and size histograms of 3 atom % Sn 12 nm ITO NCs before and after ligand exchange. Scale bars are 30 nm. (b) <sup>1</sup>H NMR spectra in CDCl<sub>3</sub> of oleic acid, as-synthesized ITO NCs, 3,5F-cinnamic acid, and 3,5F-capped ITO NCs (from top to bottom), in which line broadening indicates ligand binding on the surface. The resonance peak at 7.26 ppm corresponds to residual CHCl<sub>3</sub>. (c) Cinnamic acid ligands used in this study: 4-methoxycinnamic acid (OCH<sub>3</sub>), cinnamic acid (4H), 3,5-difluorocinnamic acid (3,5F), and 4-trifluoromethylcinnamic acid (CF<sub>3</sub>). From left to right, the ligand's dipole goes from more donating to more withdrawing toward the NC surface, with the oleate dipole lying in middle of the series. The computed dipole moments of the cinnamic acid ligands in vacuum are as reported in ref 11.

modification with dipolar ligands on plasmonic doped metal oxide NCs can offer a new post-synthetic tunability handle and lead to changes in their plasmonic properties opening new routes to improving their performance for applications such as sensing, catalysis, or optoelectronic devices.<sup>19</sup>

Herein, we analyze the impact of dipolar surface ligands on the electronic structure and plasmonic properties of doped metal oxide NCs. A series of cinnamic acid ligands with different electron withdrawing and donating dipolar characters are bound to colloidal tin-doped indium oxide (ITO) NCs via ligand exchange. The electronic properties are investigated by obtaining the work function  $(\Phi)$  of the modified ITO NCs by ultraviolet photoemission spectroscopy (UPS). Our results show that the functionalized ligands with a dipole moment pointing toward the surface (donating) lower the work function while withdrawing ligands raise the work function; this trend agrees with previous reports on a wide range of materials. 1-4,11 The plasmonic properties are analyzed by optical spectroscopy of solvent-dispersed NCs, interpreted by fitting the spectra with the heterogeneous ensemble Drude approximation (HEDA) model, which extracts quantitative parameters of interest, including the free electron concentration  $(n_e)$  and depletion layer width  $(W_D)$ . Our results demonstrate that by using post-synthetic surface modification, we access combinations of electronic properties not achievable by a direct synthetic approach. In particular, we observe when changing the ligand dipoles that  $n_e$  and the volume fraction of the plasmonic NC core  $(f_e)$  are anticorrelated, contrasting with the positive correlation between these parameters when tuning dopant concentration during synthesis. 24,25 This new strategy for post-synthetically modifying  $W_D$ , in particular, opens new opportunities to customize plasmonic metal oxide NCs for applications because the depletion layer governs the electronic and optical coupling of NCs to their environment and to adjacent molecules or other NCs.

# ITO NC SYNTHESIS AND SURFACE MODIFICATION

ITO NCs 12.2  $\pm$  1.1 nm in diameter and doped with 3 atom % Sn were synthesized by slow injection followed by mass-actiondriven ligand exchange to introduce variable surface functionalization. As detailed previously<sup>26</sup> and based on methods developed by the Hutchison group, 27,28 a metal oleate precursor solution containing both tin and indium was slowly added to a reaction flask containing oleyl alcohol. To functionalize the NC surface with dipolar molecules, oleatecapped ITO NCs (As Syn) are precipitated with ethanol and redispersed in their respective cinnamic acid ligand solutions, where 4H and OCH3 were the electron-donating ligands and CF<sub>3</sub> and 3,5F were the electron-withdrawing ligands. After being stirred for 24-48 h, the NCs are precipitated by adding hexane, with the reversal of polarity indicative of a change in surface chemistry, and then redispersed in suitable polar solvents selected for each ligand (further details in the Supporting Information). The size and shape of the As Syn ITO NCs and the surface-modified ITO NCs are obtained via scanning transmission electron microscopy (STEM), with size distribution analysis (ImageJ) including at least 400 NCs (Figures 1a and S1). There is no apparent size or shape change following ligand exchange.

Proton nuclear magnetic resonance (<sup>1</sup>H NMR) spectroscopy was used to characterize the molecular layers resulting from the cinnamate ligand exchange process. NMR is commonly used to analyze ligands on NC surfaces because bound molecules have distinctly broadened spectral features that easily distinguish them from freely diffusing molecules.<sup>29–31</sup> In our case, the presence of bound cinnamate molecules after ligand exchange is evident based on the line broadening compared to the free cinnamic acids (Figures 1b and S2). A weak signal from the alkene protons of the native oleate ligands (5.3 ppm) remains, indicating that a small amount of oleic acid persists on the surface after ligand exchange. The incomplete exchange is expected because molecules with the same anchoring group (here, carboxylate) have a similar surface binding energy.<sup>32–34</sup> Nevertheless, the presence of remaining native oleates is

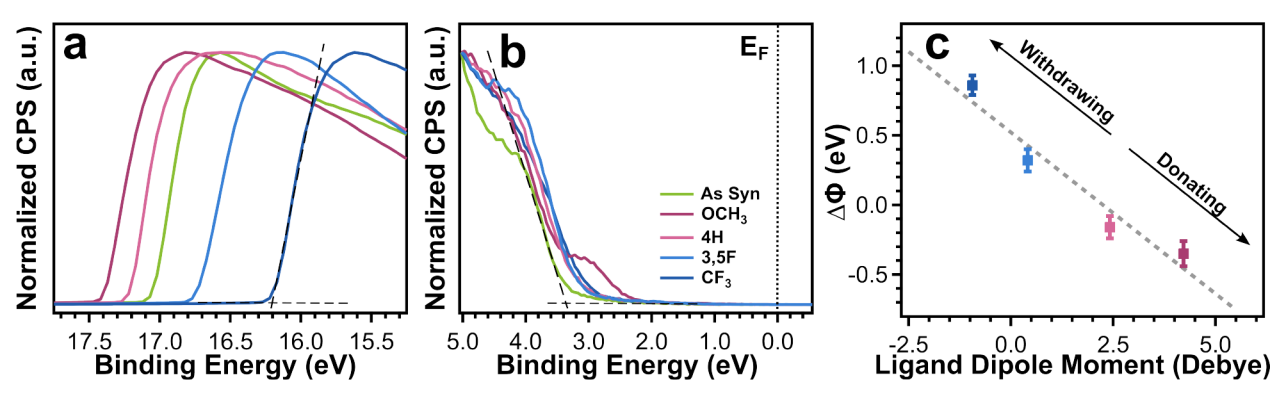


Figure 2. Electronic characterization of surface-modified ITO NCs via UPS. (a) Secondary electron cutoff region of UPS spectra. (b) Valence band maxima region of UPS spectra. (c) Change in work function with the dipole moment of cinnamic acid derivatives, shown in Figure 1c.

beneficial in promoting the colloidal stability of the cinnamate-functionalized ITO NCs. In comparison, it has been shown that phosphonic acid-terminated ligands have a stronger binding affinity to metal oxides and quantum dots, which leads to a full displacement of the native oleates.  $^{32,35-37}$  In a trial experiment, functionalizing ITO NCs with an arylphosphonic acid ligand (phenylphosphonic acid) produced a poorly dispersed colloid; therefore, we selected cinnamate ligands for this study. Ligand quantification by thermogravimetric analysis (Figures S3 and S4) gave consistent results across the dipolar series studied; after ligand exchange, the ITO NCs all have a similar cinnamate surface coverage of  $4.8 \pm 0.4$  cinnamates nm<sup>-2</sup> (see the Supporting Information text and Table S1).

#### ■ ELECTRONIC PROPERTIES

Dipolar ligands bound to a surface generate a potential energy step that changes electronic properties of the material, notably the work function  $(\Phi)$ . Dipoles commonly arise from polarization across heterointerfaces, and deliberately introducing dipoles by molecular engineering has been used to reduce onset potentials in light-emitting devices, enhance photovoltages in solar cells, and more. <sup>1,3,7-9,36,38</sup> The electrostatic effects of molecular dipole layers also influence electronic properties of nanomaterials, and they have been shown to systematically modify  $\Phi$  of colloidal quantum dots.<sup>2,10,11,14</sup> Regardless of material composition or dimensions, donating ligands produce a downward potential energy step for electrons escaping the material that lowers  $\Phi$ . Conversely, withdrawing ligands create an upward step that increases  $\Phi$ . These results have been understood based on simple electrostatics using the Helmholtz equation as an approximation,  $\Delta E = -\mu_z/(A\varepsilon_r\varepsilon_0)$ , where the change in potential energy ( $\Delta E$ ) is related to the molecular dipole moment normal to the surface  $(\mu_z)$  and the surface area per ligand molecule (A). In our case, the surface density of cinnamate ligands and the dipole arising from their bonding to the NC surface are considered to be approximately constant throughout; therefore, the dipole moment is the main variable responsible for trends in electronic and optical properties.

The impact of the molecular surface dipole on the electronic properties of ITO NCs was determined by using UPS on films of functionalized NCs. The secondary electron cutoff is used to obtain  $\Phi$  (Figure 2a), while the low binding energy region (Figure 2b) allows the determination of the ionization energy and the valence band maximum (VBM) relative to the Fermi energy ( $E_{\rm F}$ ) (Supporting Information text and Table S2).<sup>2,11</sup>

A correlation is observed between  $\Phi$  and the ligand dipole (Figure 2c). Increasing the strength of the donating ligand decreases  $\Phi$  compared to the As Syn ITO NCs, while withdrawing ligands result in higher  $\Phi$ . Between the most withdrawing (CF<sub>3</sub>) and most donating (OCH<sub>3</sub>) ligands studied  $\Phi$  varies by 1.2 eV. Similar trends and magnitudes of  $\Delta\Phi$  have been found for planar ITO films, <sup>36</sup> other bulk semiconductors, <sup>6,9</sup> and films of quantum dots. <sup>2,11</sup> Based on the Helmholtz equation, even greater changes could be anticipated for molecules with larger magnitude dipole moments or higher surface density.

Generally, changes in  $\Phi$  are caused by changes in the electron affinity or changes in the band bending, i.e., the energy difference between bulk and surface, also known as the built-in potential. Both effects have been previously reported in different semiconductor films modified by dipolar molecular layers, and they can occur simultaneously. Although UPS cannot directly differentiate these two electronic effects, the data suggest that changes in band bending are occurring for the different dipolar ligands. Specifically, if band bending remained fixed while changing  $\Phi$ , the VBM would shift identically to the secondary electron cutoff. While we do observe changes in the VBM (Figure 2b), the shifts are modest compared to changes in  $\Phi$  and they do not correlate with dipole. Thus, besides the shifts in electron affinity and ionization energy that follow the electrostatic step in the potential energy, the band bending must also be changing. Considering the importance of surface band bending for plasmonic properties of ITO NCs, 21-23 we hypothesized that functionalization with dipolar ligands should impact the spatial distribution of free electrons and the associated optical properties.

# **■ PLASMONIC PROPERTIES**

The electronic band structure of doped metal oxide NCs has a considerable impact on their plasmonic properties.  $^{22,39,40}$  For example, increasing the Sn dopant concentration during ITO NC synthesis causes a downward shift of the conduction band minimum ( $E_{\rm CBM}$ ) while filling conduction band states, leading to a larger optical gap energy (Moss–Burstein effect). However, the free electrons are not distributed uniformly throughout the NC volume because surface states pin the  $E_{\rm F}$  at the surface and induce band bending, resulting in a near-surface depletion layer. The NC volume fraction accessible to the conduction band electrons,  $f_{\rm e}$ , and their concentration within that volume,  $n_{\rm e}$ , both substantially influence plasmonic properties including the LSPR frequency, the extinction coefficient, and the near-field enhancement of resonant

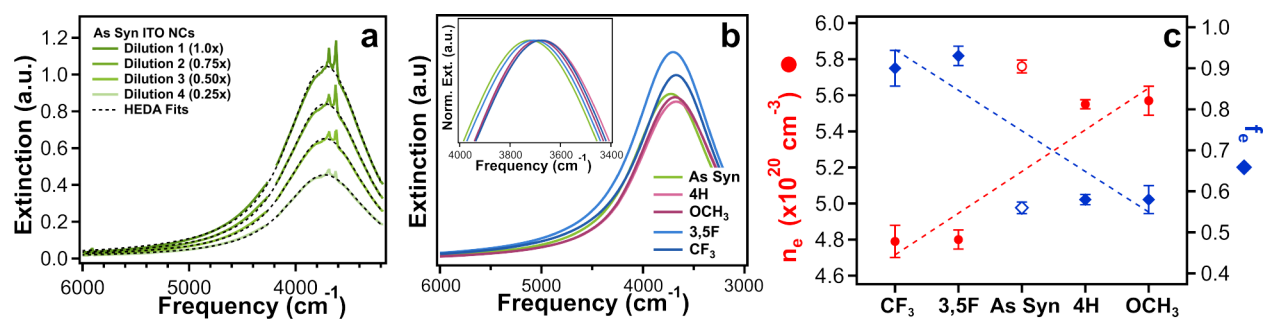


Figure 3. LSPR characteristics of surface-modified ITO NCs. (a) Measured LSPR extinction spectra of As Syn ITO NCs in dispersion at varying concentrations, fitted with the HEDA model. (b) Absolute extinction spectra, scaled with respect to the volume fraction concentration of NCs in solution, obtained from HEDA model fits for each sample of the series. The inset shows a zoom of the normalized LSPR spectra at the maximum extinction peaks to show the slight peak shifts present. (c) Electron concentration (red) and electron-accessible volume fraction (blue) for different surface ligands, in order of their dipoles from most withdrawing to most donating. Error bars represent the standard deviation in the fit results when analyzing four independently prepared dispersions with different NC concentrations.

light.<sup>21</sup> As the dopant concentration is increased, the conduction band is filled with more free electrons, causing an increase in  $n_{\rm e}$  as well as  $f_{\rm e}$ , making these plasmonic properties positively correlated for synthetically accessible variations of doped metal oxide NCs.<sup>22</sup> In this study, the UPS data suggest changes in the band bending of the ITO NCs when functionalizing their surfaces with dipolar molecules, which implies an effect on their plasmonic properties.

The LSPR frequency is significantly influenced by changes in  $n_{e_2}$  per eqs 1 and 2

$$\omega_{\rm LSPR} = \sqrt{\frac{\omega_{\rm p}^2}{\varepsilon_{\infty} + 2\varepsilon_{\rm m}} - \gamma^2}$$
 (1)

$$\omega_{\rm p} = \sqrt{\frac{n_{\rm e}e^2}{m^*\epsilon_0}} \tag{2}$$

where  $\omega_{\rm LSPR}$  and  $\omega_{\rm p}$  are the LSPR frequency and bulk plasma frequency, respectively,  $\varepsilon_{\infty}$  is the constant background polarizability of the material,  $\varepsilon_{\rm m}$  is the dielectric constant of the surrounding solvent,  $\gamma$  is the damping constant, and  $m^*$  and e are the effective mass and charge of the electrons. <sup>21</sup>

Comparing the extinction spectra of dispersed ITO NCs capped with the different cinnamic acid ligands, the magnitude of the extinction changed markedly, although the peak frequency was nearly unaffected (Figure 3b). Each sample is dispersed in a different solvent, selected to optimize colloidal stability, so variations in  $\varepsilon_{\rm m}$  may disguise any peak shifts due to changes in  $n_e$ . Although the actual peak is obscured by solvent vibrational bands, the LSPR peak maxima could be extracted by fitting (Figure 3a), and the shifts were minimal and uncorrelated to the molecular dipole (Figure S5 and Table S3). On the other hand, there is a systematic increase (decrease) in the extinction for the withdrawing (donating) functionalized NCs which indicates that the total number of free electrons per NC  $(N_e)$  has increased (decreased). With UPS suggesting changes in band bending that would impact the plasmonic properties of the NCs, determining changes that may be occurring in  $n_e$  or  $f_e$  requires more quantitative analysis of the optical spectra (Figure 3b).

Fortunately, more information can be gleaned by analyzing the LSPR spectra quantitatively using the known NC size and measured NC concentration to constrain the fitting. In the heterogeneous ensemble Drude approximation (HEDA), LSPR spectra are fit to a model that approximates the NC

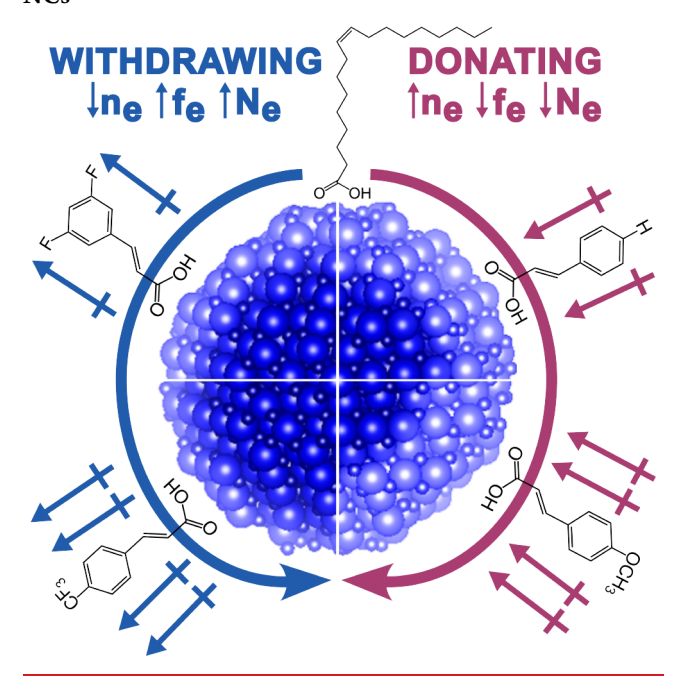
electron distribution as a metallic core surrounded by a depleted space charge layer in a core—shell structure where the plasmonic core occupies a volume fraction  $f_{\rm e}$  and contains a radially invariant electron concentration  $n_{\rm e}$ . To extract these electronic characteristics with confidence, the number of free parameters is limited by independently measuring input values, including NC concentration, size, and size distribution. To fit the measured extinction spectra to the HEDA model (Figures 3a and S5), NC sizes and size distributions obtained by STEM and concentrations of NCs in solution, determined by inductively coupled plasma-mass spectrometry, were used as fixed input parameters (further details in the Supporting Information text).

By fitting LSPR spectra with the HEDA model, we found that the electron-withdrawing (donating) ligands induce a decrease (increase) of  $n_{\rm e}$  and a larger (smaller)  $f_{\rm e}$ , which indicates a reduction (increment) of  $W_{\rm D}$  (Figure 3c). These changes in  $W_{\rm D}$  are consistent with the influence of the ligand dipoles on the band bending implicit in the UPS results. Overall, we obtain a tunability of 17% in  $n_{\rm e}$ , of 39% for  $N_{\rm e}$ , and of 66% for  $f_{\rm e}$  (Table S3). Consistent trends were found when repeating the ligand functionalization experiments with ITO NCs having different sizes and doping concentrations (Figure S6 and Table S4). Thus, the ligand dipole-induced changes in band bending are indeed evident in the NC plasmonic properties, though a cursory look at normalized LSPR spectra obscured the trends.

Together, these results indicate an anticorrelation between  $n_e$  and  $f_e$  as the ligand dipole is varied (Figure 3c and Scheme 1). Because raising  $n_e$  by synthetically boosting the Sn concentration or growing larger NCs also increases  $f_e$ . This anticorrelation is uniquely accessible by post-synthetic ligand exchange. Such a combination of properties suggests new opportunities to design NCs for specific applications. For example, electron-withdrawing ligands enable access to NCs with a low  $n_e$ , which can facilitate the generation of hot electrons, while reducing  $W_D$  to allow rapid extraction of those excited electrons.

There are two possible mechanisms by which a molecular layer on a semiconductor surface modifies band bending, and both are related to the surface states: state mixing, which is based on surface state hybridization, and static fields, which is based on electrostatics. <sup>12,42</sup> First, in the state mixing case, the change in band bending is driven by the interaction between the material's surface states and the molecular LUMO level of

Scheme 1. Summarized Results Relating Surface Modification Impacts to the Plasmonic Properties of ITO NCs



the ligand, producing hybridized states. Hybridization shifts the filled surface states to lower energy, causing a change in band bending. If this mechanism was governing the influence of dipolar molecules on ITO NCs, we would expect to see that for electron-withdrawing ligands, as the LUMO level of the ligand is lower in energy, 43,44 the band bending will become more significant due to better energetic alignment with the surface states. However, this is the opposite of the observed trend because our experiments revealed diminished band bending for more withdrawing ligands. Therefore, the state mixing mechanism is inconsistent with our results. In the static field mechanism, the change in band bending results from the molecular dipole-derived step in the potential energy. If this mechanism was governing our observations, we would expect that the downward electrostatic potential step induced by donating ligands would increase band bending, while the upward step associated with withdrawing ligands would

decrease band bending (Figure 4). In the experimental data, we see this exact trend in which withdrawing (donating) ligands result in a decrease (increase) of the band bending of the material, producing the observed effects on the plasmonic properties. Furthermore, an increase (decrease) in optical gap occurs for NCs functionalized with withdrawing (donating) ligands (Figure S7), in agreement with the expected change in energy difference from  $E_{\rm VBM}$  to  $E_{\rm F}$  (Figure 4). All of these observed trends are consistent with those expected based on the static fields mechanism, indicating that field effects dominate in determining the influence of dipolar ligand functionalization on the electronic and plasmonic properties of ITO NCs.

In conclusion, we demonstrated that post-synthetically modifying ITO NCs with dipolar ligands changes their electronic band structure and tunes the electron concentration and radial distribution. Dipolar ligands systematically increase or decrease band bending, causing the electron concentration and plasmonic volume fraction to vary in an anticorrelated manner. Post-synthetic surface modification can provide access to combinations of plasmonic properties that cannot be achieved by direct synthetic routes like changing size and doping density.<sup>25</sup> Considering the two known mechanisms that can explain how a molecular layer influences band bending, our data suggest that the static field mechanism based on electrostatics is dominant in this case. In future studies, direct observations of the surface state energies, e.g., with energyresolved electrochemical impedance spectroscopy, 45,46 and direct analysis of the band bending, e.g., with angle-resolved photoemission spectroscopy,<sup>18</sup> may be used to further analyze the influence of dipolar ligands, ligands with different binding groups, 47,48 and other surface chemical modifications. Furthermore, the influence of dipolar ligands on plasmonic properties of other semiconductor NCs, such as doped ZnO, 49,50 CdO, 51 and p-type copper chalcogenide NCs, 5 each having distinct electronic structure and band bending characteristics, would broaden understanding of the properties and phenomena we observed here for ITO NCs.2

#### ASSOCIATED CONTENT

#### Supporting Information

The Supporting Information is available free of charge at https://pubs.acs.org/doi/10.1021/acs.nanolett.3c01943.

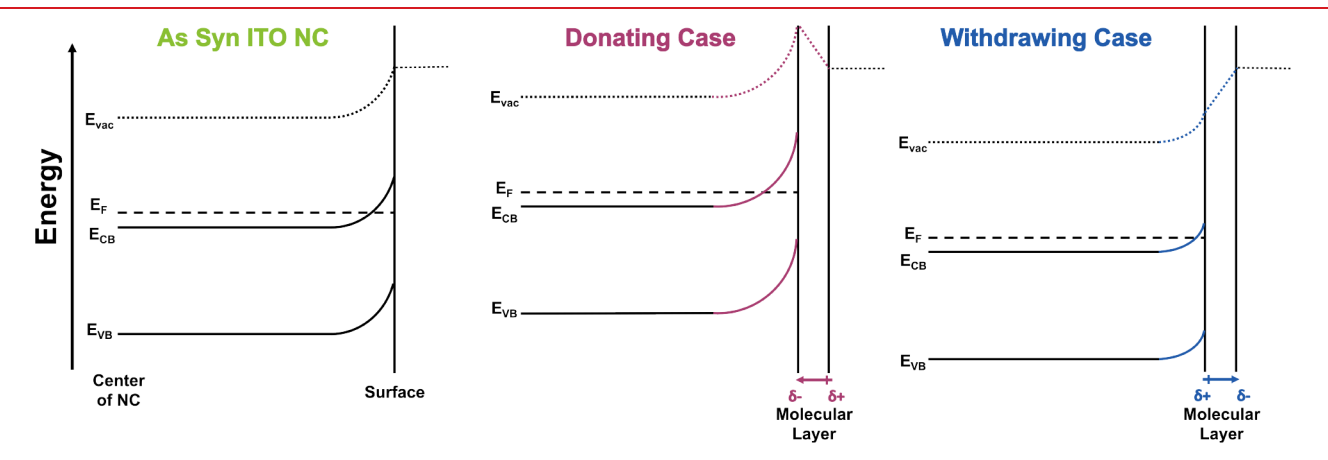


Figure 4. Schematic representation of the changes in the band bending of ITO NCs depending on the dipolar character of the surface ligands. The modified band bending in the depletion layer is highlighted with colored lines extending the conduction  $(E_{CB})$  and valence band edges  $(E_{VB})$  radially out from the center of the NC and the potential steps in the molecular layers are shown by the change in the vacuum level  $(E_{Vac})$ .

Details of ITO NC synthesis, surface modification procedure, and characterization techniques used (STEM, NMR, TGA, UPS, optical spectroscopy, ICP-MS, and HEDA model) for all samples, plus supporting characterization data (PDF)

# AUTHOR INFORMATION

#### **Corresponding Author**

Delia J. Milliron – Department of Chemistry and McKetta Department of Chemical Engineering, University of Texas at Austin, Austin, Texas 78712, United States; orcid.org/ 0000-0002-8737-451X; Email: milliron@che.utexas.edu

#### Authors

- Victor Segui Barragan Department of Chemistry, University of Texas at Austin, Austin, Texas 78712, United States; orcid.org/0009-0001-5600-5535
- Benjamin J. Roman McKetta Department of Chemical Engineering, University of Texas at Austin, Austin, Texas 78712, United States; oorcid.org/0000-0003-2213-2533
- Sofia A. Shubert-Zuleta Department of Chemistry, University of Texas at Austin, Austin, Texas 78712, United States; orcid.org/0000-0003-0445-175X
- Marina W. Berry Department of Chemistry, University of Texas at Austin, Austin, Texas 78712, United States Hugo Celio – Texas Materials Institute, University of Texas at Austin, Austin, Texas 78712, United States

Complete contact information is available at: https://pubs.acs.org/10.1021/acs.nanolett.3c01943

### **Notes**

The authors declare no competing financial interest.

# ACKNOWLEDGMENTS

The authors acknowledge support from the National Science Foundation (NSF) (CHE-1905263), the Welch Foundation (F-1848), and the NSF Graduate Research Fellowship Program (DGE-2137420). Partial support was also provided by the Center for Dynamics and Control of Materials, an NSF Materials Research Science and Engineering Center under Cooperative Agreement DMR-1720595.

## REFERENCES

- (1) Zehner, R. W.; Parsons, B. F.; Hsung, R. P.; Sita, L. R. Tuning the Work Function of Gold with Self-Assembled Monolayers Derived from  $X-[C_6H_4-C-C-]_nC_6H_4$ -SH (n = 0, 1, 2; X = H, F, CH<sub>3</sub>, CF<sub>3</sub>, and OCH<sub>3</sub>). *Langmuir* **1999**, *15*, 1121–1127.
- (2) Brown, P. R.; Kim, D.; Lunt, R. R.; Zhao, N.; Bawendi, M. G.; Grossman, J. C.; Bulović, V. Energy Level Modification in Lead Sulfide Quantum Dot Thin Films through Ligand Exchange. *ACS Nano* **2014**, *8*, 5863–5872.
- (3) Vilan, A.; Ghabboun, J.; Cahen, D. Molecule Metal Polarization at Rectifying GaAs Interfaces. J. Phys. Chem. B 2003, 107, 6360–6376.
- (4) Cahen, D.; Kahn, A. Electron Energetics at Surfaces and Interfaces: Concepts and Experiments. *Adv. Mater.* **2003**, *15*, 271–277.
- (5) Bruening, M.; Moons, E.; Cahen, D.; Shanzer, A. Controlling the Work Function of CdSe by Chemisorption of Benzoic Acid Derivatives and Chemical Etching. *J. Phys. Chem.* **1995**, *99*, 8368–8373.
- (6) Krüger, J.; Bach, U.; Grätzel, M. Modification of  ${\rm TiO_2}$  Heterojunctions with Benzoic Acid Derivatives in Hybrid Molecular Solid-State Devices. *Adv. Mater.* **2000**, *12*, 447–451.

- (7) Vilan, A.; Shanzer, A.; Cahen, D. Molecular control over Au/GaAs diodes. *Nature* **2000**, *404*, 166–168.
- (8) Wu, D. G.; Ghabboun, J.; Martin, J. M. L.; Cahen, D. Tuning of Au/n-GaAs Diodes with Highly Conjugated Molecules. *J. Phys. Chem. B* **2001**, *105*, 12011–12018.
- (9) Ashkenasy, G.; Cahen, D.; Cohen, R.; Shanzer, A.; Vilan, A. Molecular Engineering of Semiconductor Surfaces and Devices. *Acc. Chem. Res.* **2002**, *35*, 121–128.
- (10) Chuang, C.-H. M.; Brown, P. R.; Bulović, V.; Bawendi, M. G. Improved performance and stability in quantum dot solar cells through band alignment engineering. *Nat. Mater.* **2014**, *13*, 796–801.
- (11) Kroupa, D. M.; Vörös, M.; Brawand, N. P.; McNichols, B. W.; Miller, E. M.; Gu, J.; Nozik, A. J.; Sellinger, A.; Galli, G.; Beard, M. C. Tuning colloidal quantum dot band edge positions through solution-phase surface chemistry modification. *Nat. Commun.* **2017**, *8*, 15257.
- (12) Vilan, A.; Cahen, D. Chemical Modification of Semiconductor Surfaces for Molecular Electronics. *Chem. Rev.* **2017**, *117*, 4624–4666
- (13) Prather, K. V.; Stoffel, J. T.; Tsui, E. Y. Redox Reactions at Colloidal Semiconductor Nanocrystal Surfaces. *Chem. Mater.* **2023**, 35, 3386–3403.
- (14) Crisp, R. W.; Kroupa, D. M.; Marshall, A. R.; Miller, E. M.; Zhang, J.; Beard, M. C.; Luther, J. M. Metal Halide Solid-State Surface Treatment for High Efficiency PbS and PbSe QD Solar Cells. *Sci. Rep.* **2015**, *5*, 9945.
- (15) Rhee, S.; Hahm, D.; Seok, H.-J.; Chang, J. H.; Jung, D.; Park, M.; Hwang, E.; Lee, D. C.; Park, Y.-S.; Kim, H.-K.; Bae, W. K. Steering interface dipoles for bright and efficient all-inorganic quantum dot based light-emitting diodes. *ACS Nano* **2021**, *15*, 20332–20340.
- (16) Ozawa, K.; Emori, M.; Yamamoto, S.; Yukawa, R.; Yamamoto, S.; Hobara, R.; Fujikawa, K.; Sakama, H.; Matsuda, I. Electron—hole recombination time at  $TiO_2$  single-crystal surfaces: Influence of surface band bending. *J. Phys. Chem. Lett.* **2014**, *5*, 1953–1957.
- (17) Hikita, Y.; Nishio, K.; Seitz, L. C.; Chakthranont, P.; Tachikawa, T.; Jaramillo, T. F.; Hwang, H. Y. Band Edge Engineering of Oxide Photoanodes for Photoelectrochemical Water Splitting: Integration of Subsurface Dipoles with Atomic-Scale Control. *Adv. Energy Mater.* **2016**, *6*, 1502154.
- (18) Sato, S.; Kataoka, K.; Jinnouchi, R.; Takahashi, N.; Sekizawa, K.; Kitazumi, K.; Ikenaga, E.; Asahi, R.; Morikawa, T. Band bending and dipole effect at interface of metal-nanoparticles and  ${\rm TiO_2}$  directly observed by angular-resolved hard X-ray photoemission spectroscopy. *Phys. Chem. Phys.* **2018**, *20*, 11342–11346.
- (19) Agrawal, A.; Cho, S. H.; Zandi, O.; Ghosh, S.; Johns, R. W.; Milliron, D. J. Localized Surface Plasmon Resonance in Semi-conductor Nanocrystals. *Chem. Rev.* **2018**, *118*, 3121–3207.
- (20) Liyanage, T.; Nagaraju, M.; Johnson, M.; Muhoberac, B. B.; Sardar, R. Reversible tuning of the plasmoelectric effect in noble metal nanostructures through manipulation of organic ligand energy levels. *Nano Lett.* **2020**, *20*, 192–200.
- (21) Gibbs, S. L.; Staller, C. M.; Milliron, D. J. Surface Depletion Layers in Plasmonic Metal Oxide Nanocrystals. *Acc. Chem. Res.* **2019**, 52, 2516–2524.
- (22) Zandi, O.; Agrawal, A.; Shearer, A. B.; Reimnitz, L. C.; Dahlman, C. J.; Staller, C. M.; Milliron, D. J. Impacts of surface depletion on the plasmonic properties of doped semiconductor nanocrystals. *Nat. Mater.* **2018**, *17*, 710–717.
- (23) Ghini, M.; Curreli, N.; Lodi, M. B.; Petrini, N.; Wang, M.; Prato, M.; Fanti, A.; Manna, L.; Kriegel, I. Control of electronic band profiles through depletion layer engineering in core—shell nanocrystals. *Nat. Commun.* **2022**, *13*, 537.
- (24) Tandon, B.; Gibbs, S. L.; Zydlewski, B. Z.; Milliron, D. J. Quantitative Analysis of Plasmonic Metal Oxide Nanocrystal Ensembles Reveals the Influence of Dopant Selection on Intrinsic Optoelectronic Properties. *Chem. Mater.* **2021**, *33*, 6955–6964.
- (25) Gibbs, S. L.; Staller, C. M.; Agrawal, A.; Johns, R. W.; Saez Cabezas, C. A.; Milliron, D. J. Intrinsic Optical and Electronic Properties from Quantitative Analysis of Plasmonic Semiconductor

- Nanocrystal Ensemble Optical Extinction. J. Phys. Chem. C 2020, 124, 24351–24360.
- (26) Staller, C. M.; Gibbs, S. L.; Saez Cabezas, C. A.; Milliron, D. J. Quantitative Analysis of Extinction Coefficients of Tin-Doped Indium Oxide Nanocrystal Ensembles. *Nano Lett.* **2019**, *19*, 8149–8154.
- (27) Jansons, A. W.; Hutchison, J. E. Continuous Growth of Metal Oxide Nanocrystals: Enhanced Control of Nanocrystal Size and Radial Dopant Distribution. *ACS Nano* **2016**, *10*, 6942–6951.
- (28) Crockett, B. M.; Jansons, A. W.; Koskela, K. M.; Johnson, D. W.; Hutchison, J. E. Radial Dopant Placement for Tuning Plasmonic Properties in Metal Oxide Nanocrystals. *ACS Nano* **2017**, *11*, 7719–7728.
- (29) Hens, Z.; Martins, J. C. A Solution NMR Toolbox for Characterizing the Surface Chemistry of Colloidal Nanocrystals. *Chem. Mater.* **2013**, 25, 1211–1221.
- (30) Marbella, L. E.; Millstone, J. E. NMR Techniques for Noble Metal Nanoparticles. *Chem. Mater.* **2015**, *27*, 2721–2739.
- (31) De Roo, J.; Yazdani, N.; Drijvers, E.; Lauria, A.; Maes, J.; Owen, J. S.; Van Driessche, I.; Niederberger, M.; Wood, V.; Martins, J. C.; Infante, I.; Hens, Z. Probing Solvent—Ligand Interactions in Colloidal Nanocrystals by the NMR Line Broadening. *Chem. Mater.* **2018**, *30*, 5485—5492.
- (32) Knauf, R. R.; Lennox, J. C.; Dempsey, J. L. Quantifying Ligand Exchange Reactions at CdSe Nanocrystal Surfaces. *Chem. Mater.* **2016**, 28, 4762–4770.
- (33) Kessler, M. L.; Starr, H. E.; Knauf, R. R.; Rountree, K. J.; Dempsey, J. L. Exchange equilibria of carboxylate-terminated ligands at PbS nanocrystal surfaces. *Phys. Chem. Chem. Phys.* **2018**, 20, 23649–23655.
- (34) Smock, S. R.; Williams, T. J.; Brutchey, R. L. Quantifying the Thermodynamics of Ligand Binding to CsPbBr<sub>3</sub> Quantum Dots. *Angew. Chem., Int. Ed.* **2018**, *57*, 11711–11715.
- (35) Lee, J. T.; Hati, S.; Fahey, M. M.; Zaleski, J. M.; Sardar, R. Surface-Ligand-Controlled Enhancement of Carrier Density in Plasmonic Tungsten Oxide Nanocrystals: Spectroscopic Observation of Trap-State Passivation via Multidentate Metal Phosphonate Bonding. Chem. Mater. 2022, 34, 3053–3066.
- (36) Hotchkiss, P. J.; Jones, S. C.; Paniagua, S. A.; Sharma, A.; Kippelen, B.; Armstrong, N. R.; Marder, S. R. The Modification of Indium Tin Oxide with Phosphonic Acids: Mechanism of Binding, Tuning of Surface Properties, and Potential for Use in Organic Electronic Applications. *Acc. Chem. Res.* **2012**, *45*, 337–346.
- (37) Paniagua, S. A.; Hotchkiss, P. J.; Jones, S. C.; Marder, S. R.; Mudalige, A.; Marrikar, F. S.; Pemberton, J. E.; Armstrong, N. R. Phosphonic Acid Modification of Indium-Tin Oxide Electrodes: Combined XPS/UPS/Contact Angle Studies. *J. Phys. Chem. C* 2008, 112, 7809–7817.
- (38) Cohen, R.; Kronik, L.; Shanzer, A.; Cahen, D.; Liu, A.; Rosenwaks, Y.; Lorenz, J. K.; Ellis, A. B. Molecular Control over Semiconductor Surface Electronic Properties: Dicarboxylic Acids on CdTe, CdSe, GaAs, and InP. *J. Am. Chem. Soc.* **1999**, *121*, 10545–10553.
- (39) Hamberg, I.; Granqvist, C. G.; Berggren, K. F.; Sernelius, B. E.; Engström, L. Band-gap widening in heavily Sn-doped In<sub>2</sub> O<sub>3</sub>. *Phys. Rev. B* **1984**, *30*, 3240–3249.
- (40) Berggren, K. F.; Sernelius, B. E. Band-gap narrowing in heavily doped many-valley semiconductors. *Phys. Rev. B* **1981**, *24*, 1971–1986.
- (41) Johns, R. W.; Blemker, M. A.; Azzaro, M. S.; Heo, S.; Runnerstrom, E. L.; Milliron, D. J.; Roberts, S. T. Charge carrier concentration dependence of ultrafast plasmonic relaxation in conducting metal oxide nanocrystals. *J. Mater. Chem. C* **2017**, *5*, 5757–5763.
- (42) Neale, N. R.; Pekarek, R. T. Springer Handbook of Inorganic Photochemistry; Springer Handbooks: 2022; pp 923–964.
- (43) Cohen, R.; Bastide, S.; Cahen, D.; Libman, J.; Shanzer, A.; Rosenwaks, Y. Controlling electronic properties of CdTe by adsorption of dicarboxylic acid derivatives: Relating molecular

- parameters to band bending and electron affinity changes. *Adv. Mater.* **1997**, *9*, 746–749.
- (44) Rangan, S.; Batarseh, A.; Chitre, K. P.; Kopecky, A.; Galoppini, E.; Bartynski, R. A. Tuning Energy Level Alignment At Organic/Semiconductor Interfaces Using a Built-In Dipole in Chromophore—Bridge—Anchor Compounds. *J. Phys. Chem. C* **2014**, *118*, 12923—12928
- (45) Volk, S.; Yazdani, N.; Sanusoglu, E.; Yarema, O.; Yarema, M.; Wood, V. Measuring the Electronic Structure of Nanocrystal Thin Films Using Energy-Resolved Electrochemical Impedance Spectroscopy. *J. Phys. Chem. Lett.* **2018**, *9*, 1384–1392.
- (46) Volk, S.; Yazdani, N.; Yarema, O.; Yarema, M.; Bozyigit, D.; Wood, V. In Situ Measurement and Control of the Fermi Level in Colloidal Nanocrystal Thin Films during Their Fabrication. *J. Phys. Chem. Lett.* **2018**, *9*, 7165–7172.
- (47) Balitskii, O. A.; Sytnyk, M.; Stangl, J.; Primetzhofer, D.; Groiss, H.; Heiss, W. Tuning the Localized Surface Plasmon Resonance in Cu<sub>2-x</sub> Se Nanocrystals by Postsynthetic Ligand Exchange. *ACS Appl. Mater. & Interfaces* **2014**, *6*, 17770–17775.
- (48) Balitskii, O.; Mashkov, O.; Barabash, A.; Rehm, V.; Afify, H. A.; Li, N.; Hammer, M. S.; Brabec, C. J.; Eigen, A.; Halik, M.; et al. Ligand Tuning of Localized Surface Plasmon Resonances in Antimony-Doped Tin Oxide Nanocrystals. *Nanomaterials* **2022**, *12*, 3469
- (49) Della Gaspera, E.; Chesman, A. S.; Van Embden, J.; Jasieniak, J. J. Non-injection synthesis of doped zinc oxide plasmonic nanocrystals. *ACS Nano* **2014**, *8*, 9154–9163.
- (50) Buonsanti, R.; Llordes, A.; Aloni, S.; Helms, B. A.; Milliron, D. J. Tunable infrared absorption and visible transparency of colloidal aluminum-doped zinc oxide nanocrystals. *Nano Lett.* **2011**, *11*, 4706–4710.
- (51) Gordon, T. R.; Paik, T.; Klein, D. R.; Naik, G. V.; Caglayan, H.; Boltasseva, A.; Murray, C. B. Shape-dependent plasmonic response and directed self-assembly in a new semiconductor building block, indium-doped cadmium oxide (ICO). *Nano Lett.* **2013**, *13*, 2857–2863.
- (52) Xu, W.; Liu, H.; Zhou, D.; Chen, X.; Ding, N.; Song, H.; Ågren, H. Localized surface plasmon resonances in self-doped copper chalcogenide binary nanocrystals and their emerging applications. *Nano Today* **2020**, *33*, 100892.